A study of the anomalous behavior of the

electrical resistivity in alloys near

the $PrNi_{5.0}$ composition

by

Weol Dong Cho

A Thesis Submitted to the

Graduate Faculty in Partial Fulfillment of the

Requirements for the Degree of

MASTER OF SCIENCE

Department: Materials Science and Engineering

Major: Metallurgy

Iowa State University
Ames, Iowa

1982

TABLE OF CONTENTS

I. INTRODUCTION

Studies of the physical and chemical properties of praseodymium intermetallic compounds are of great interest because the compounds can be used as a nuclear refrigerant to reach millikelvin (mK) temperatures.

It is difficult to cool samples into the low millikelvin region. Three methods for cooling to 10 mK or lower are available. These are the ^{3}He/^{4}He dilution refrigeration, Pomeranchuk cooling, and adiabatic nuclear demagnetization. By means of nuclear demagnetization, a spin temperature of 0.2 µK has been reached, while conduction electron has been cooled to 0.4 mK. When improved, this method will permit one to make many types of experiments in the millikelvin region.

One variation of the nuclear demagnetization is the so-called hyperfine enhanced nuclear demagnetization. This method was theoretically predicted by Al'tshuler (1) and first put into practice by Andres and Bucher (2). Hyperfine enhanced nuclear magnetic cooling is based on the fact that in singlet ground state ions with high Van Vleck magnetic susceptibilities, large hyperfine fields can be induced by moderate external fields. To obtain a high enhancement value a small separation between the singlet ground state and the first excited state is needed. This leads to a

high Van Vleck susceptibility. The larger the Van Vleck susceptibility, the smaller the exchange interaction between neighboring ions.

Among the rare earth ions Pr^{3+} is the logical choice because it has the lowest spin angular momentum, a singlet ground state, and a fairly large Van Vleck susceptibility. Also, because of the enhancement factor, fairly large reduction in the nuclear entropy of Pr can be obtained with moderate magnetic field.

Therefore, many praseodymium intermetallic compounds have been studied by physicists. Recently, Andres, Bucher and others have shown that some of the intermetallic compounds of praseodymium are useful refrigerants for producing temperatures of the order of 1 mK or below (3). Magnetic moments of intermetallic compounds formed between a transition metal and a rare-earth element were investigated by Nesbitt et al. (4). They found that, except for $PrNi_5$, all RNi_5 (R = rare - earth) compounds are ferromagnetic or antiferromagnetic at low temperatures. Sugawara et al. (5) measured the fracture strength, thermal conductivity and electrical resistivity of $PrCu_6$, $PrNi_5$, $PrPt_5$ and $PrIn_3$. They could not measure the thermal conductivity of $PrNi_5$ because of its brittleness. Meijer et al. (6) electroplated $PrNi_5$ with copper to improve the mechanical

property and found some advantages in machining the samples after electroplating.

One of the most suitable compounds is $PrNi_5$ which was first investigated as nuclear refrigerant by Andres and co-workers [7]. Andres and Darack [8] were the first to use the Van Vleck paramagnet $PrNi_5$, and reached a temperature of 0.2 mK by demagnetizing this compound.

Recently, Folle et al. [9] have performed extensive adiabatic refrigeration experiments with $PrNi_5$. They showed that $PrNi_5$ has a nuclear ferromagnetic ordering transition at (0.4 ± 0.02) mK and they have reached a minimum temperature of 0.2 mK by demagnetizing $PrNi_5$. Low temperature thermal expansion coefficient and specific heat of $PrNi_5$ were measured by Ott et al. [10].

$PrNi_5$ crystallizes in the hexagonal $CaCu_5$-type structure and the intermetallic compound appears to melt congruently as it forms readily from the melt. All Pr ions are in equivalent sites and experience a crystal field of hexagonal symmetry. Each Pr ion is surrounded by a hexagon of six nearest Ni ions in the same plane and by two hexagons of six next-nearest Ni ions above and below this plane.

Wernick and Geller [11] investigated the structural properties of intermetallic compounds between rare-earth and transition elements including $PrNi_5$ which have the

$CaCu_5$ structure. Wernick and Geller pointed out that the rare earth atoms do not interact at all in the c-axis direction, i.e. the arrangement of atoms of transition elements only need to be modified in the basal planes to accommodate rare earth atoms of different size.

Dwight (12) studied about the interrelations of atomic size, stacking geometry and electronic structure of 27 AB_5 $CaCu_5$-type intermetallic compounds. He obtained the lattice parameters of $\underline{a}o = 4.64(A°)$, $\underline{c}o = 3.975(A°)$ for $PrNi_5$. He noted that A atom is always larger in AB_5 $CaCu_5$-type compounds and that the compounds exist when the component metals have radius ratio in the range from 1.29 to 1.61.

Mueller (13) pointed out an anomaly in electrical resistivity of $PrNi_{5.0}$, in that the room temperature resistivities were increased by about 10-20% after the samples had been cooled to helium temperature. More recently, the temperature dependence of the electrical resistivity and thermal conductivity of $PrNi_{5.0}$ was investigated by Reiffers et al. (14). They also found that the electrical resistivity had higher values after repeated cooling cycles and the thermal conductivity decreased by almost a factor of two after about 20 cycles. They observed an inflection point around 10 K in the temperature dependence of the electrical resistivity, which was also confirmed by Craig et al. (15).

The change of the slope at the inflection point in the resistivity vs. temperature curve was suggested by Craig et al. to be due to the effect of crystal-fields on the resistivity.

The purpose of this study of the electrical resistivities in Pr-Ni alloy system was to examine the anomalous behavior reported earlier by Mueller et al. (13) and Reiffers et al. (14). Temperature, composition, and heat treatment dependence of resistivity of $PrNi_x$ were studied and the effect of thermal cycling was examined.

If it is assumed that the contribution to the resistivity from the lattice vibrations is independent of the residual resistivity, then the total resistivity can be written according to Mattheissen's rule as

$$\rho = \rho_r + \rho_i$$

where ρ_r is the residual resistivity which is temperature independent and due to lattice defects and impurities, and ρ_i is the ideal resistivity which is temperature dependent and due to scattering of the electrons by the lattice vibrations.

Since an electron moves freely through a perfect lattice without disturbance, the resistance only becomes finite when we take into account the irregularities in the lattice structure. The most important factor in producing

irregularities is usually the thermal motion of the metallic ions, but impurities, strains, point and line defect, etc. also play a role which is especially evident at low temperature.

The thermal vibrations of the lattice produce a resistance which is normally much larger than that due to the impurities and/or defects, but it diminishes rapidly as the temperature is lowered so that at sufficiently low temperature the resistance becomes independent of the temperature. Since this residual resistance is due to impurities, strains, displaced atoms, voids, etc., it varies from specimen to specimen. If the residual resistance is subtracted from the total resistance a quantity is obtained called the ideal resistance which is assumed to be characteristic of pure metal and due to the thermal vibrations only.

II. SAMPLE PREPARATION

The Pr used for this study is made at the Ames Labora-
tory. Ni was purchased from International Nickel Company.
The impurities in Pr and Ni were analyzed by spark source
mass spectrometric method. The impurities in Pr and Ni are
given in Tables 1 and 2, respectively.

Table 1. Elemental impurities in Pr (atomic ppm)[a]

Impurity		Impurity	
H	<139	Fe	18
C	47	Nb	<5
N	<10	Ta	29
O	141	La	3.4
F	<22	Ce	6
Al	2	Nd	3
Si	10	Gd	2.1
Cl	10	Ir	<2
Ti	1.1	Pt	<10

[a]Only impurity levels greater than 1 atomic ppm are
listed.

Before weighing, the Pr rod was electropolished to re-
move surface oxide scale. The appropriate quantities of
each element were weighed and then arc-melted under Ar
atmosphere to make rod-shape samples. To improve homo-
geneity of the samples, they were repeatedly melted about

Table 2. Elemental impurities in Ni (atomic ppm)[a]

Impurity		Impurity	
H	<50	Zr	<2
C	540	Nb	<20
N	<4	Sn	<2
O	26	Ce	<2
Si	10	Gd	<9
P	<4	Dy	<2
Cl	2	Hf	<3
Cr	1	W	<2
Fe	3	Os	<2
Co	<2		

[a]Only impurity levels greater than 1 atomic ppm are listed.

five times and were turned over after each melt.

Initially, six compositions were made by arc-melting - $PrNi_{4.6}$, $PrNi_{4.7}$, $PrNi_{4.8}$, $PrNi_{4.9}$, $PrNi_{5.0}$, $PrNi_{5.2}$; and later, in order to examine the composition range from 4.9 to 5.0 in more detail, samples of $PrNi_{4.93}$, $PrNi_{4.96}$ and $PrNi_{4.98}$ were prepared. At the beginning of this research, attempts were made to prepare samples of $PrNi_{5.4}$ and $PrNi_{5.6}$ compositions by arc-melting. But useful resistivity samples could not be prepared because of their brittleness. After arc-melting, as the rods cooled they broke into several large pieces which had many cracks.

After arc-melting, the good rod-shaped samples were cut with diamond saw to make rectangular samples for measuring the electrical resistivity. Final shaping for exact rectangular samples was accomplished by carefully sanding with No. 600 sand paper because of brittleness of samples.

Part of each as-cast sample was used for electrical resistivity. The rest of each as-cast samples was used for heat-treatment. For annealing, the samples were sealed in Ta tubes by arc-welding under Ar atmosphere, and then the tubes were placed in quartz capsules which were sealed under Ar atmosphere. The quartz capsules were maintained in the furnace at various temperatures. The samples were heat-treated at 1000°C, 1100°C, and 1200°C for a week and then rapidly quenched in ice water. Five samples except for $PrNi_{5.2}$ were heat-treated at 1200°C. But only $PrNi_{5.0}$ sample was good. The other four samples partially melted because of the Pr_2Ni_7 peritectic temperature at >1100°C. After quenching, the electrical resistivities were measured.

A portion of each as-cast and quenched samples was used for metallography. The samples for metallography were mechanically polished with No. 600 sand paper and then electrolytically polished. Nital was used as an ethant. All of the photomicrographs were taken at 250 magnification.

III. EXPERIMENTAL PROCEDURES

Electrical resistivity measurements were made over the temperature range from 300 to 4.2 K by the standard dc four probe technique and were calculated by the formula

$$\rho = \frac{V}{I} \frac{A}{L}$$

where ρ is the electrical resistivity ($\mu\Omega$cm), V is the voltage (μV) measured between the probes, I is the current (mA) flowing through the sample with a cross sectional area of A, and L is the distance between the voltage probes. A constant dc current source was used and the measurements were taken with the current in both directions and the values were averaged.

The temperature was determined by measuring the voltage from one of two types of thermocouples. For temperatures above 70 K a constantan/copper thermocouple was used and for temperatures below 70 K a Au-Fe/Cu thermocouple was used. At low temperatures Au-Fe/Cu thermocouple is more sensitive to temperature changes than constantan/copper thermocouple.

The temperature is controlled by passing the current through a manganin heater. The heater current was determined by a proportional temperature controller, using a carbon re-sistor as the sensing element between 4.2 K and 30 K because below 30 K it has a large resistance. At higher tempera-

tures the resistance of the carbon resistor is too large, so, a copper resistor was used as the sensing element at the temperatures between 30 K and 300 K.

Electrical resistivity was measured in a continuous fashion on cooling and heating. Each sample was measured through at least a second cooling and heating cycle in order to examine the effect of thermocycling.

X-ray diffraction powder patterns of the 1000°C heat-treated samples were taken using Debye-Scherrer cameras. The samples were exposed for 12 hours to Cu Kα radiation. Most of the back-reflection lines were not well-resolved. The ao and co parameters were obtained from an extrapolation of the back-reflection data determined by least-squares methods.

Photomicrographs of each alloy composition in the as-cast and various heat-treated stages were taken before and after thermal cycling.

IV. RESULTS

Electrical resistivities of $PrNi_x$ samples were measured from 300 K to 4.2 K and from 4.2 K to 300 K using liquid nitrogen and helium as the coolants. The alloy compositions studied were for x = 4.6, 4.7, 4.8, 4.9, 5.0 and 5.2. The samples of each composition were made in as-casting and heat-treated plus quenching from 1000°C, 1100°C and 1200°C.

The electrical resistivity increases monotonically with increasing temperature as shown in Figures 1-4. Figure 1 shows the temperature dependence of the resistivities of $PrNi_{4.8}$ and $PrNi_{5.2}$, which were quenched from 1100°C. The data were taken on slow cooling and heating from 300 K to 4.2 K and back to 300 K. As shown in Figure 1, there is a kink point in $PrNi_{5.2}$ around 30 K. It is probably due to severe cracking which occurred over a narrow temperature range. This kink in the resistivity is not due to magnetic ordering because it is not seen in the heating curve nor is it evident in the second cooling and heating cycle, see Figure 2. It is evident from metallographic examination that for x ≥ 5.2 many cracks were observed in the samples after the first cooling-heating cycle. Furthermore, it is noted that the higher Ni concentration, the more cracks per unit area.

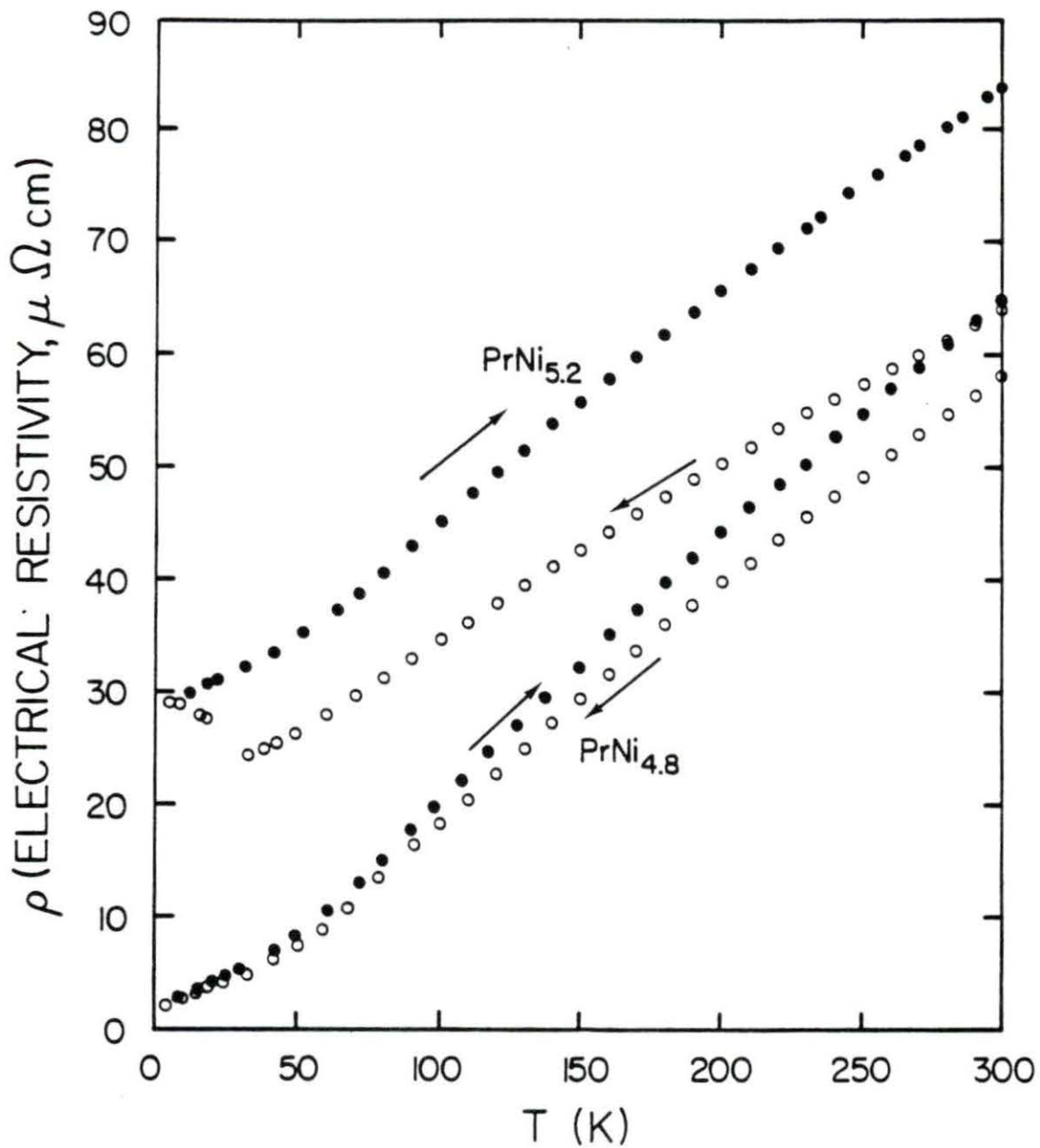Figure 2 shows second thermal cycle of samples shown

Figure 1. Temperature dependence of electrical resisitivity on the initial cooling and heating cycle of $PrNi_{4.8}$ and $PrNi_{5.2}$ which were quenched from 1100°C
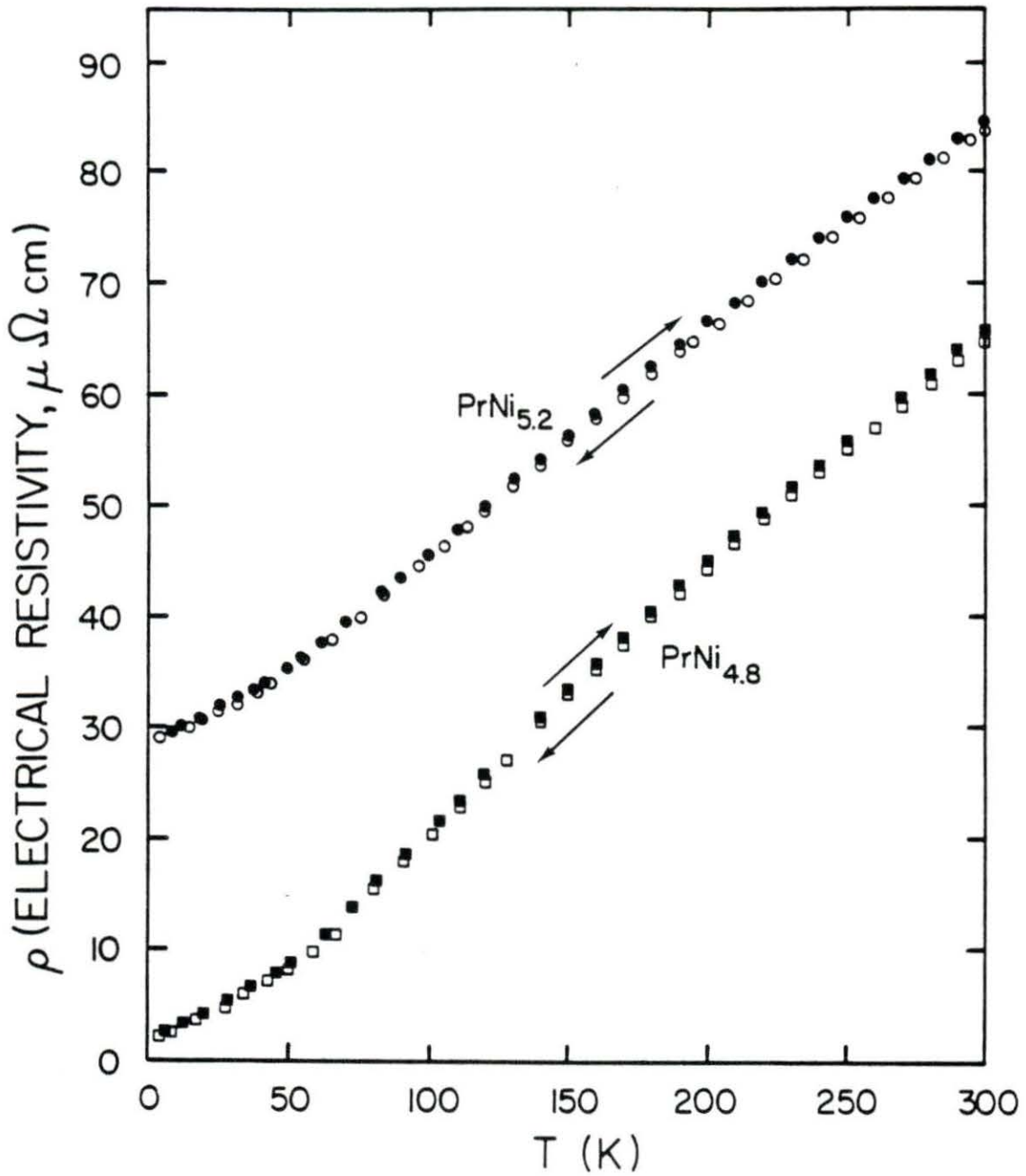
Figure 2. Second cooling and heating process of PrNi$_{4.8}$ and PrNi$_{5.2}$ which are quenched from 1100°C. The open data points were taken on cooling and the solid points were taken on heating
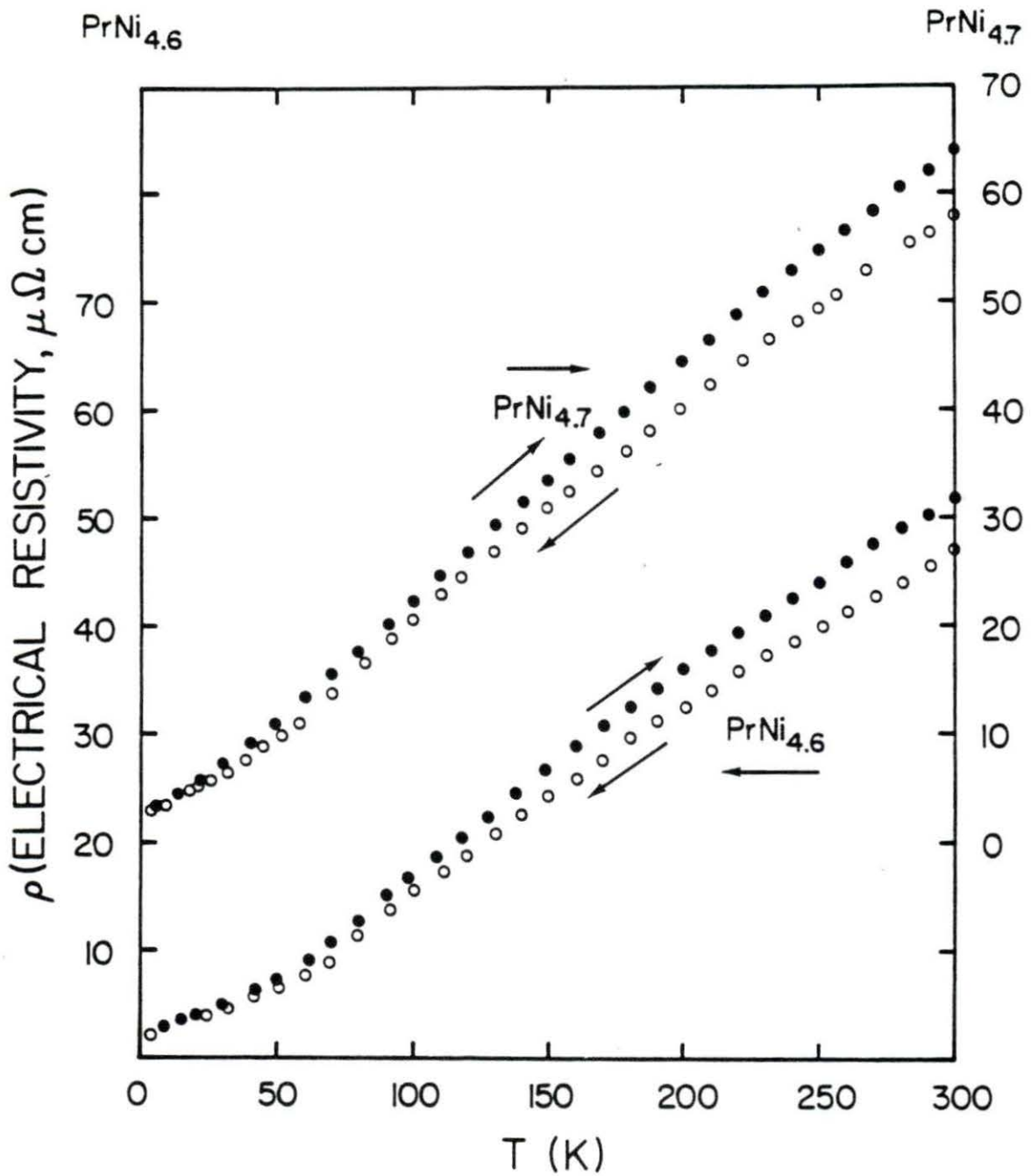
Figure 3. Temperature dependence of electrical resistivity of
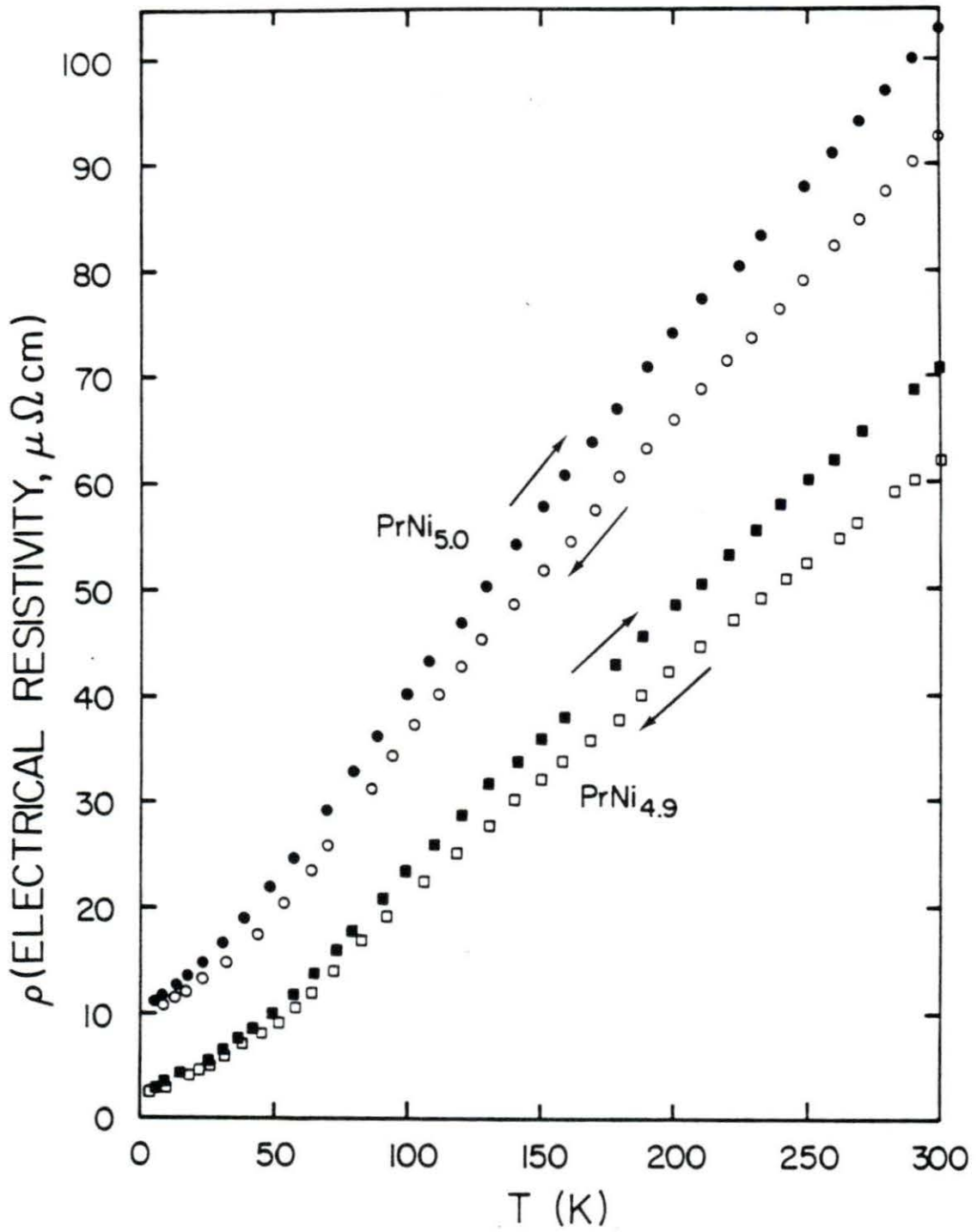PrNi$_{4.6}$ and PrNi$_{4.7}$ which are quenched from 1100°C

Figure 4. Temperature dependence of electrical resistivity
of PrNi$_{4.9}$ and PrNi$_{5.0}$ which are quenched from
1100°C

in Figure 1. For the second cooldown, there is only a slight increase in the resistivity values, especially when compared to the difference after the first cycle (Figure 1). Furthermore, since there is little change in the resistivity from the first heating curve to subsequent cycles, it is concluded that most of the cracking occurs on the initial cooling, and little thereafter.

Figures 3 and 4 show the first thermal cycle of $PrNi_{4.6}$, $PrNi_{4.7}$, $PrNi_{4.9}$ and $PrNi_{5.0}$. As seen in the figures, the resistivities increased with increasing nickel concentrations. Also, it is noted that the difference in the resistivity ($\Delta\rho$) between the initial room temperature value and that at room temperature after the first complete cycle increases with increasing nickel content, see Figure 5. Since the increase in $\Delta\rho$ is thought to be proportional to the number of cracks which developed upon cooling, then one would conclude that the higher nickel content alloys have a larger number of cracks per unit volume, which is consistent with metallographic observations noted earlier.

The data for each of the samples are summarized in Tables 3, 4 and 5. Usually, the resistivities of heat-treated samples are lower than those of as-casted samples. This point will be discussed later.

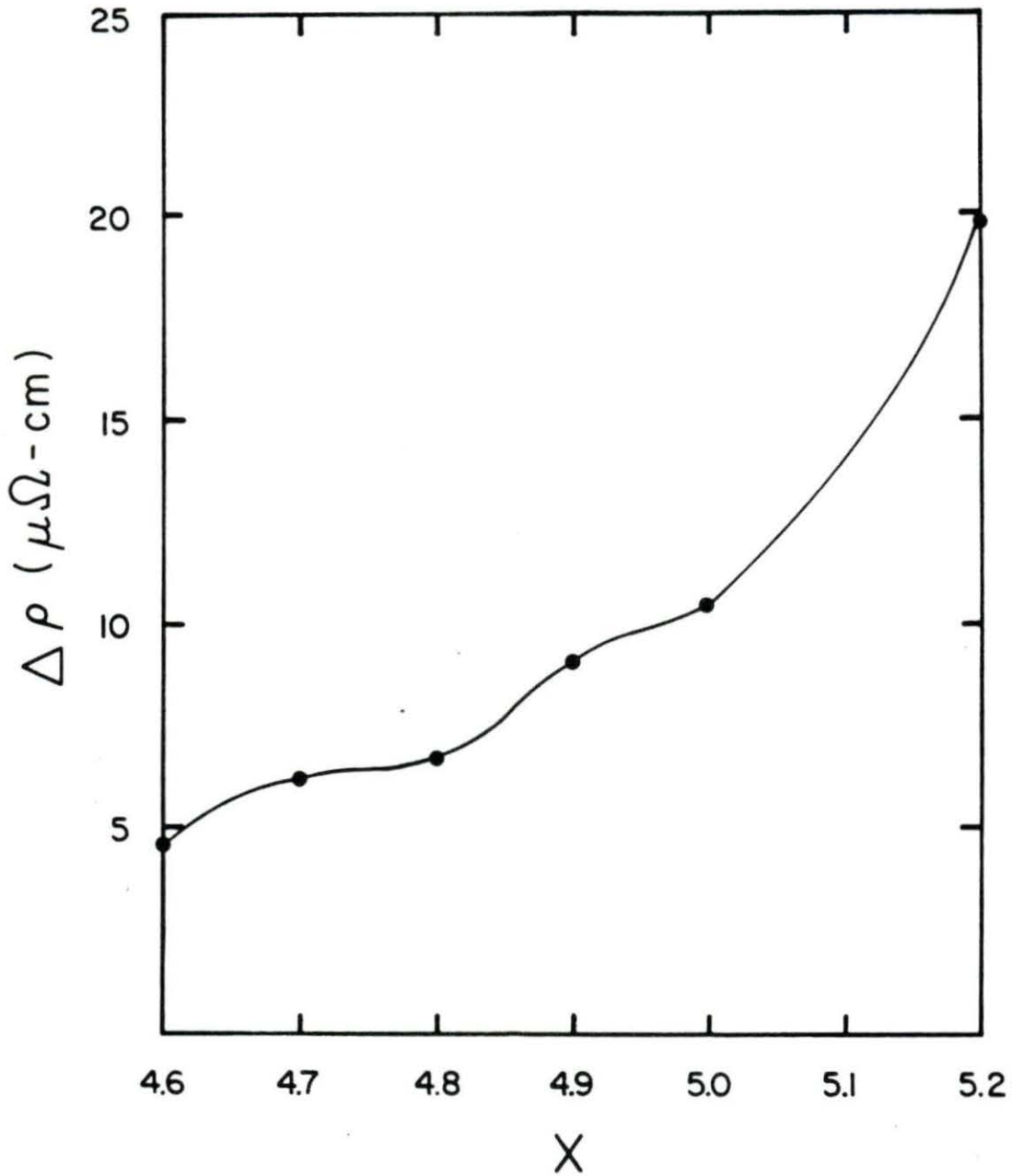Composition dependence of resistivities of first cycle

Figure 5. Compositional dependence of the room temperature
resistivity difference (Δρ) between before and
after first thermal cycle for the samples which
were quenched from 1100°C

Table 3. The electrical resistivity (ρ) and residual resistivity ratio ($\Gamma_{4.2}$) of as-cast $PrNi_x$

Composition	1st cooling			1st heating		2nd cooling			2nd heating	
	ρ_{300}	$\rho_{4.2}$	$\Gamma_{4.2}$	ρ_{300}	$\Gamma_{4.2}$	ρ_{300}	$\rho_{4.2}$	$\Gamma_{4.2}$	ρ_{300}	$\Gamma_{4.2}$
$PrNi_{4.6}$	52.96	3.2	16.55	64.40	20.13	64.68	3.43	18.86	61.50	19.68
$PrNi_{4.7}$	56.52	1.95	28.98	63.42	32.52	63.61	2.04	31.18	64.39	31.50
$PrNi_{4.8}$	66.33	3.02	21.96	77.32	25.60	77.28	3.04	25.59	78.48	25.9
$PrNi_{4.9}$	61.45	2.10	29.26	70.63	33.63	70.53	2.13	33.11	72.39	33.99
$PrNi_{5.0}$	77.00	5.02	15.34	26.50	17.23	86.72	5.52	15.07	87.87	15.47
$PrNi_{5.2}$	113.90	37.91	3.00	124.29	3.28	124.47	38.80	2.56	125.72	3.24

Table 4. The electrical resistivity (ρ) and residual resistivity ratio ($\Gamma_{4.2}$) of PrNi$_x$ which were quenched from 1000°C

Composition	1st cooling			1st heating		2nd cooling			2nd heating	
	ρ_{300}	$\rho_{4.2}$	$\Gamma_{4.2}$	ρ_{300}	$\Gamma_{4.2}$	ρ_{300}	$\rho_{4.2}$	$\Gamma_{4.2}$	ρ_{300}	$\Gamma_{4.2}$
PrNi$_{4.6}$	40.83	2.27	17.99	42.62	18.78	43.78	2.20	19.90	43.55	19.80
PrNi$_{4.7}$	54.60	3.46	15.78	62.88	18.17	62.98	3.52	17.89	64.12	18.22
PrNi$_{4.8}$	44.79	1.89	23.70	52.79	27.93	52.90	1.88	28.14	53.63	28.53
PrNi$_{4.9}$	59.70	3.97	15.04	69.90	17.61	69.90	4.03	17.34	71.07	17.64
PrNi$_{5.0}$	66.70	4.53	14.72	75.50	16.67	78.00	4.60	16.96	78.50	17.07
PrNi$_{5.2}$	82.30	24.00	3.43	100.27	4.18	100.75	28.00	3.60	102.36	3.66

Table 5. The electrical resistivity (ρ) and residual resitivity ratio ($\Gamma_{4.2}$) of $PrNi_x$ which were quenched from 1100°C

Composition	1st cooling			1st heating		2nd cooling			2nd heating	
	ρ_{300}	$\rho_{4.2}$	$\Gamma_{4.2}$	ρ_{300}	$\Gamma_{4.2}$	ρ_{300}	$\rho_{4.2}$	$\Gamma_{4.2}$	ρ_{300}	$\Gamma_{4.2}$
$PrNi_{4.6}$	47.00	2.12	22.17	51.64	24.36	51.73	2.10	24.63	52.38	24.94
$PrNi_{4.7}$	57.93	3.02	19.18	64.05	21.21	64.07	3.00	21.36	63.66	21.22
$PrNi_{4.8}$	58.18	2.14	27.19	64.79	30.28	64.85	2.10	30.88	65.88	31.36
$PrNi_{4.9}$	61.81	2.68	23.06	70.71	26.38	70.64	2.70	26.16	71.04	26.31
$PrNi_{5.0}$	92.69	10.68	8.68	103.12	9.66	102.78	10.78	9.53	105.63	9.80
$PrNi_{5.2}$	63.98	29.15	2.19	83.78	2.87	83.78	29.19	2.87	84.59	2.90

of as-casted and heat-treated samples is shown in Figure 6.
In general, the room temperature resistivity increases with
increasing x. The maximum room temperature resistivity ob-
served was 126 $\mu\Omega$cm for x = 5.2 of as-casted sample, and
the minimum was 44 $\mu\Omega$cm for x = 4.6 of 1000°C heat-treated
sample. The residual resistivities exhibit a minimum of
1.9 $\mu\Omega$cm for x = 4.8 for the 1000°C heat-treated sample, and
a maximum of 38 $\mu\Omega$cm for x = 5.2 for the as-casted sample.
The residual resistivity results for the as-cast samples
are similar to those of Sugawara et al. (5). After thermal
cycling, the residual resistivities are slightly increased.
For x ≥ 5.0, the residual and room temperature resistivities
increased because of cracks developing in these brittle
materials.

The 10-20% increase in the room temperature resis-
tivities after the samples were cooled once to helium
temperature was already noted by Mueller et al. (13). Also,
Reiffers et al. (14) found out that the thermal conductivity
decreased almost two times after about 20 cycles. As noted
earlier, we believe that the reason for these two phenomena
is probably due to the development of cracks during thermal
cycling. By comparing the photomicrographs taken before and
after thermal cycling, it was seen that new cracks developed
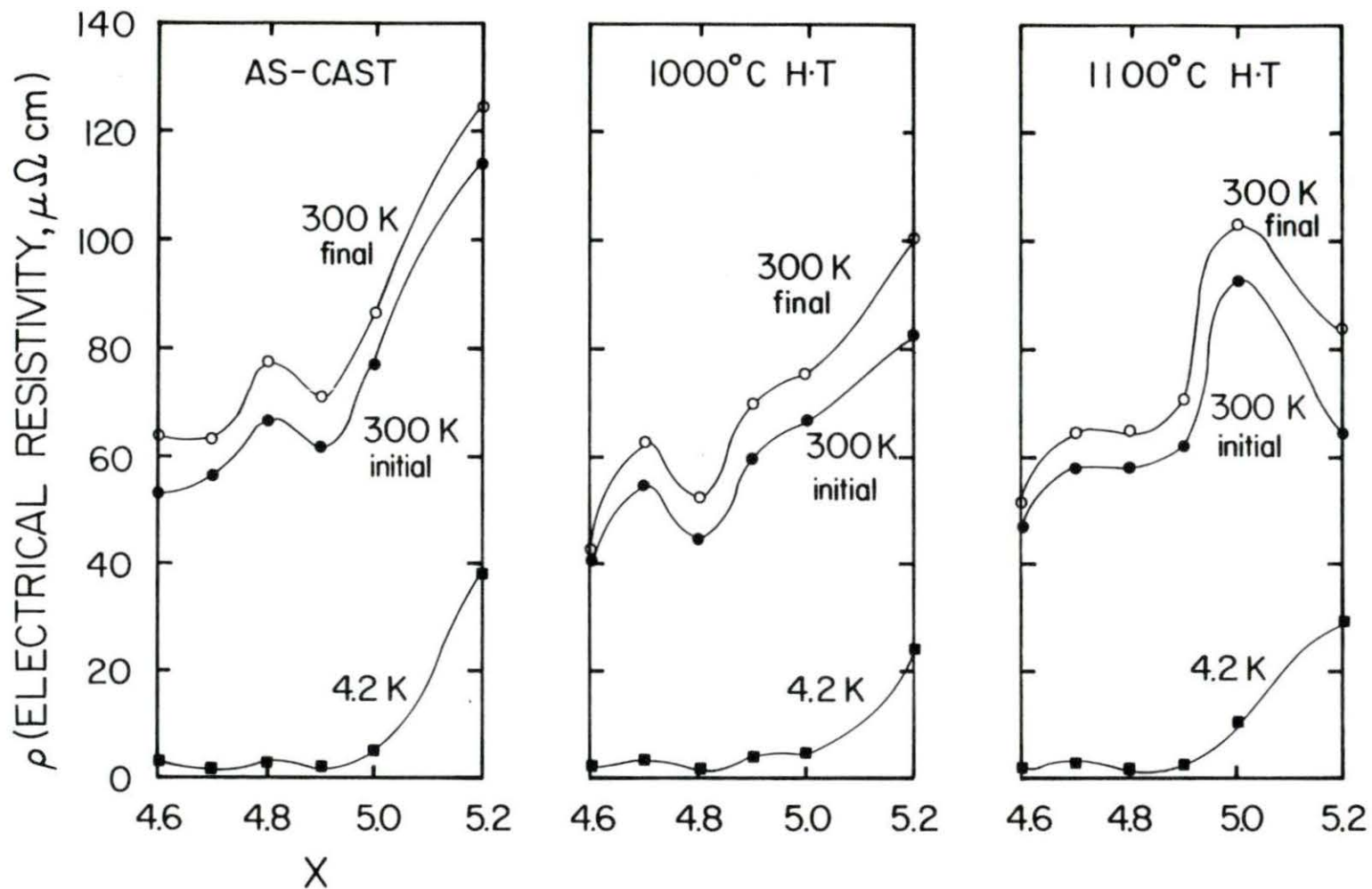or that additional cracks were formed in samples during

Figure 6. Composition dependence of electrical resistivity. Open circles represent values after one complete thermal cycle. Closed circles represent the values taken before cooling the samples. Closed squares are the 4.2 K values taken in the initial cooling-heating cycle

thermal cycling, see Figures 7 and 8. Most cracks are
transgranular but some follow the grain boundaries. Many
slip lines were also noted in the alloys near the x = 5
composition, see Figure 9.

Figure 10 shows composition vs. residual resistivity
ratio $(\rho_{300}/\rho_{4.2})$. The maximum ratio is 34 at x = 4.9 of
as-casted sample and the minimum is 3 at x = 5.2 of 1100°C
heat-treated sample. The residual resistivity ratio is in-
creased by about 10-20% after first cooling because of in-
creasing the room temperature resistivity. For x ≥ 5.0, the
residual resistivity ratio is quite small because of the
high residual resistivity in these alloys. Compositional
dependence of residual resistivity ratio of as-casted
samples is different from those of heat-treated samples,
i.e. heat-treated samples have maximum ratio at x = 4.8 but
as-casted samples have local minimum at x = 4.8. This
probably results from inhomogeneity of as-casted samples or
possibly the loss of one of the components during arc-
melting or a weighing error in making up the alloys.

The dependence of the electrical resistivity on the
heat treatment conditions of $PrNi_{5.0}$ is shown in Figure 11.
The sample quenched from 1000°C has lowest residual and
room temperature resistivity and the sample quenched from
1200°C has highest residual resistivity.

(a)   (b)
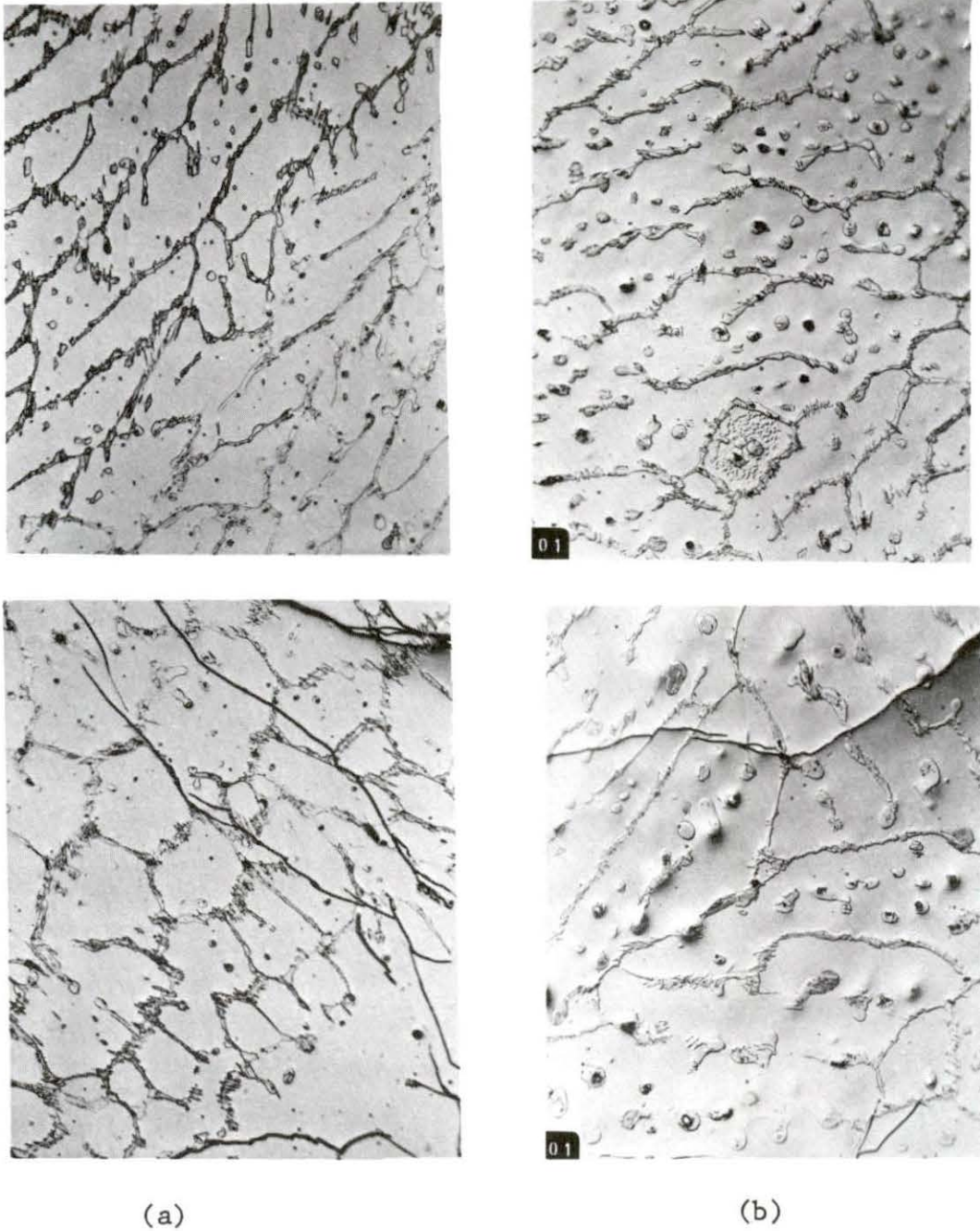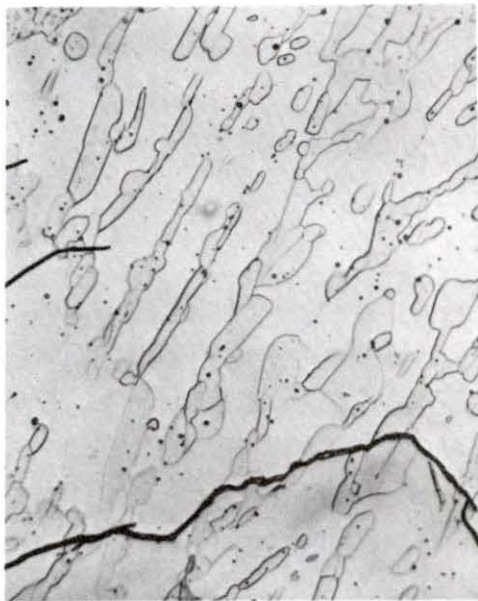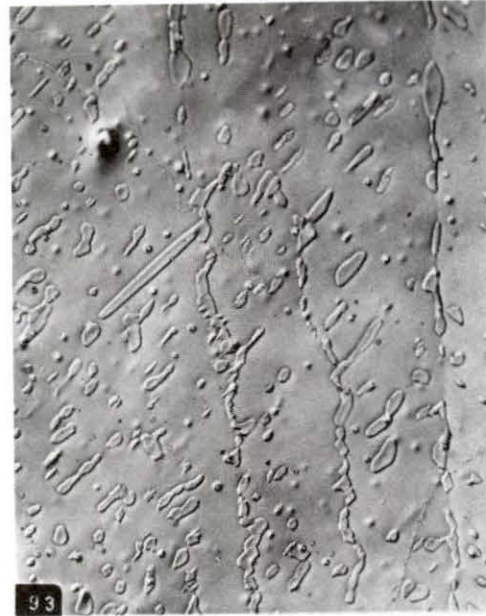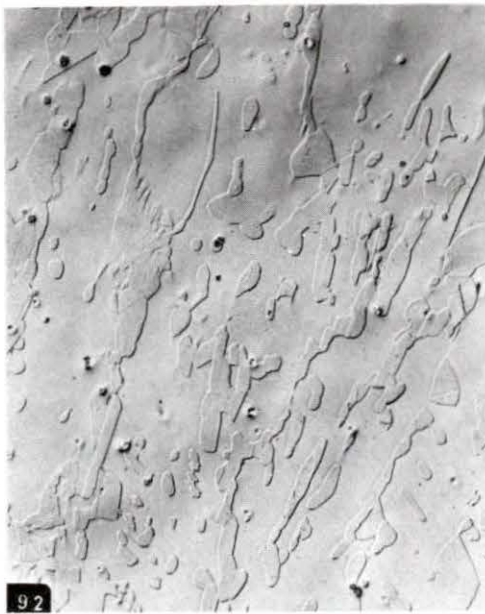
Figure 7(a).   Metallography of as-casted PrNi$_{4.8}$ before (top)
                and after (bottom) thermal cycling (x250)

         (b)   Metallography of as-casted PrNi$_{4.7}$ before (top)
                and after (bottom) thermal cycling (x250)

(a)   (b)

Figure 8(a).   Metallography of 1100°C heat-treated PrNi$_{4.6}$
               before (top) and after (bottom) thermal
               cycling (x250)

      8(b).   Metallography of 1100°C heat-treated PrNi$_{4.8}$
               (top) and after (bottom) thermal cycling
               (x250)

(a)

(b)

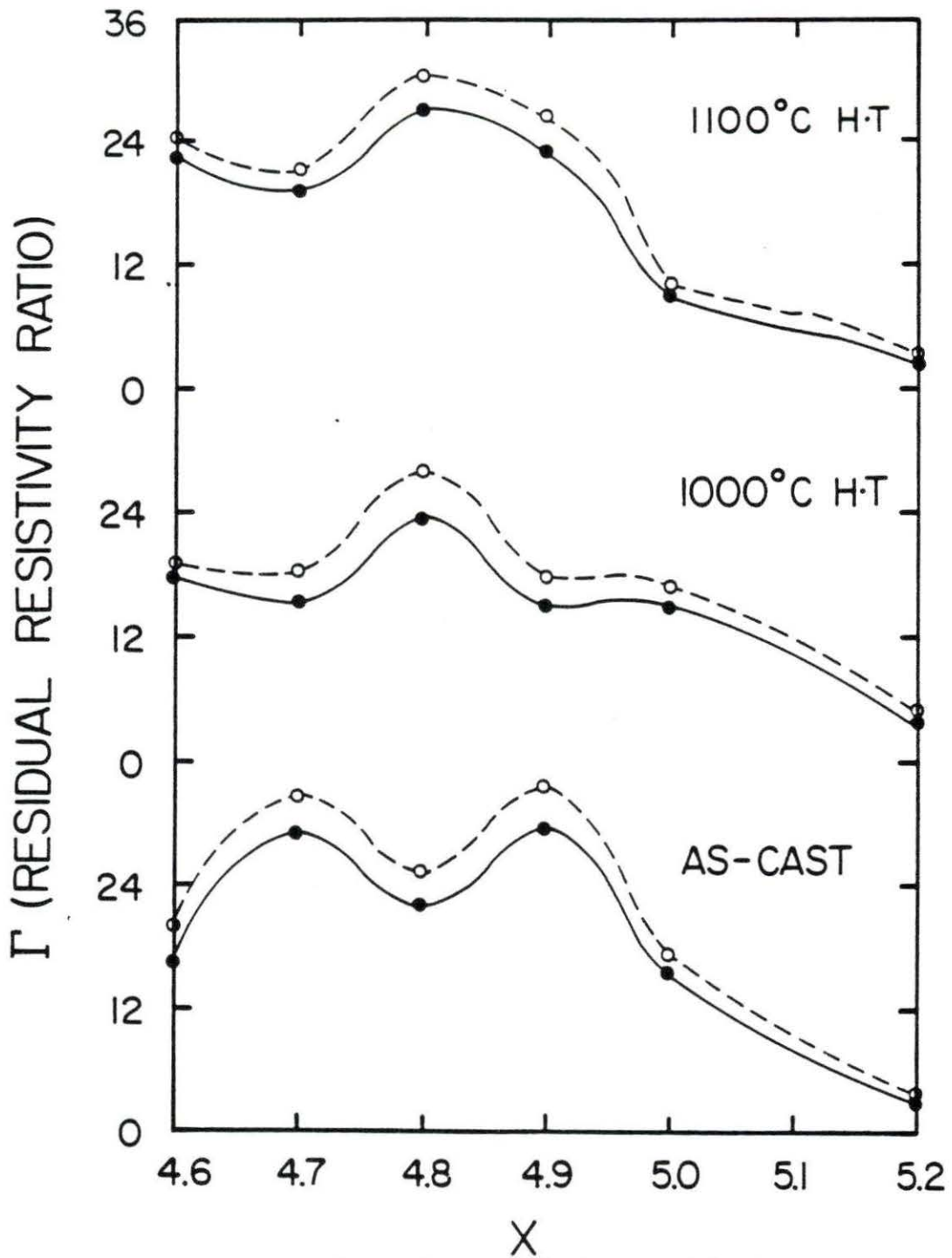Figure 9. Metallography of as-casted PrNi$_{4.96}$ (a) and PrNi$_{4.98}$ after thermal cycling (x250)

Figure 10. Composition dependence of the residual resistivity ratio for the PrNi$_x$ alloys. Open circles represent the values obtained after first complete cycle. The solid points are the values based on the initial room temperature resistivity values
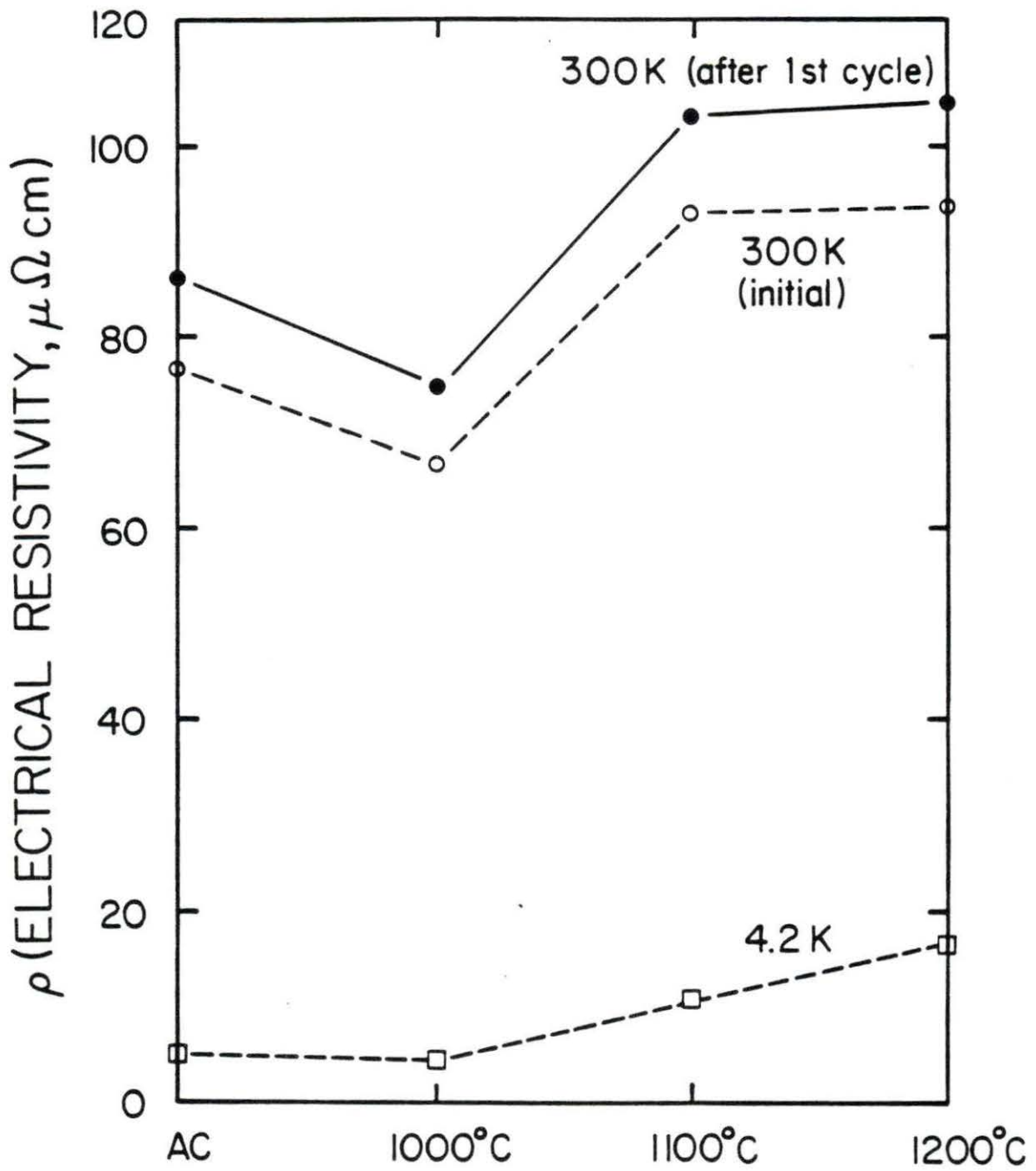
Figure 11. Heat-treatment dependence of electrical resis-
tivity of PrNi$_{5.0}$. Open squares are residual
resistivity

Metallographic examination of all the as-casted samples revealed that only $PrNi_{5.0}$ is a single phase alloy. For $x > 5$, the samples consist of $PrNi_{5.0}$ and Ni and for $x < 5$, $PrNi_{5.0}$ and Pr_2Ni_7. As a result of quenching from 1000°C, the homogeneity region is broader, i.e. $PrNi_{5.0}$ and $PrNi_{5.2}$ are single phase alloys. Of the samples quenched from 1100°C, only the $PrNi_{5.0}$ sample is a single phase alloy. For samples heat treated at 1200°C, all samples except $PrNi_{5.0}$ melted because the eutectic temperatures on both sides of this compound are <1200°C.

Photomicrographs of the as-casted $PrNi_{5.2}$ and $PrNi_{5.4}$ alloys show a fine Ni precipitate at the grain boundary and inside the grain. Figure 12 shows that precipitation has occurred primarily at the grain boundary in the 1000°C heat-treated $PrNi_{5.4}$ and $PrNi_{5.6}$ samples. The eutectic between $PrNi_{5.0}$ and Ni is shown in Figure 13 for the $PrNi_{5.2}$ alloy which was quenched from 1100°C. For the samples with $x < 5.0$ and which lie in the two phase region, almost all of the quenched samples show the agglomeration of liquid at the grain boundary and inside the grain.

The variation of the unit cell dimensions for the samples, which were quenched from 1000°C, was studied by x-ray diffraction. The lattice constant as a function of the composition for $PrNi_x$ is shown in Figure 14. As men-

(a)
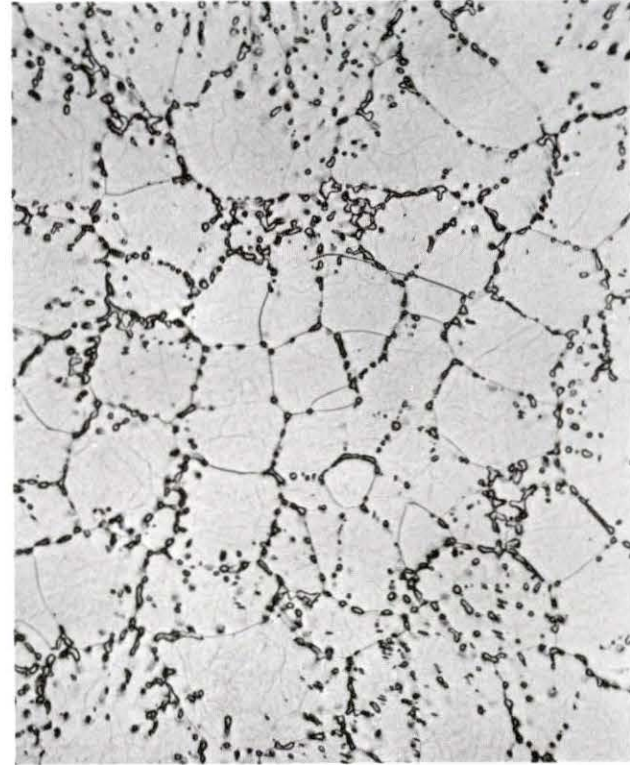
(b)

Figure 12. Metallography of PrNi$_{5.4}$ (a) and PrNi$_{5.6}$ (b) quenched from
1100°C (x250)

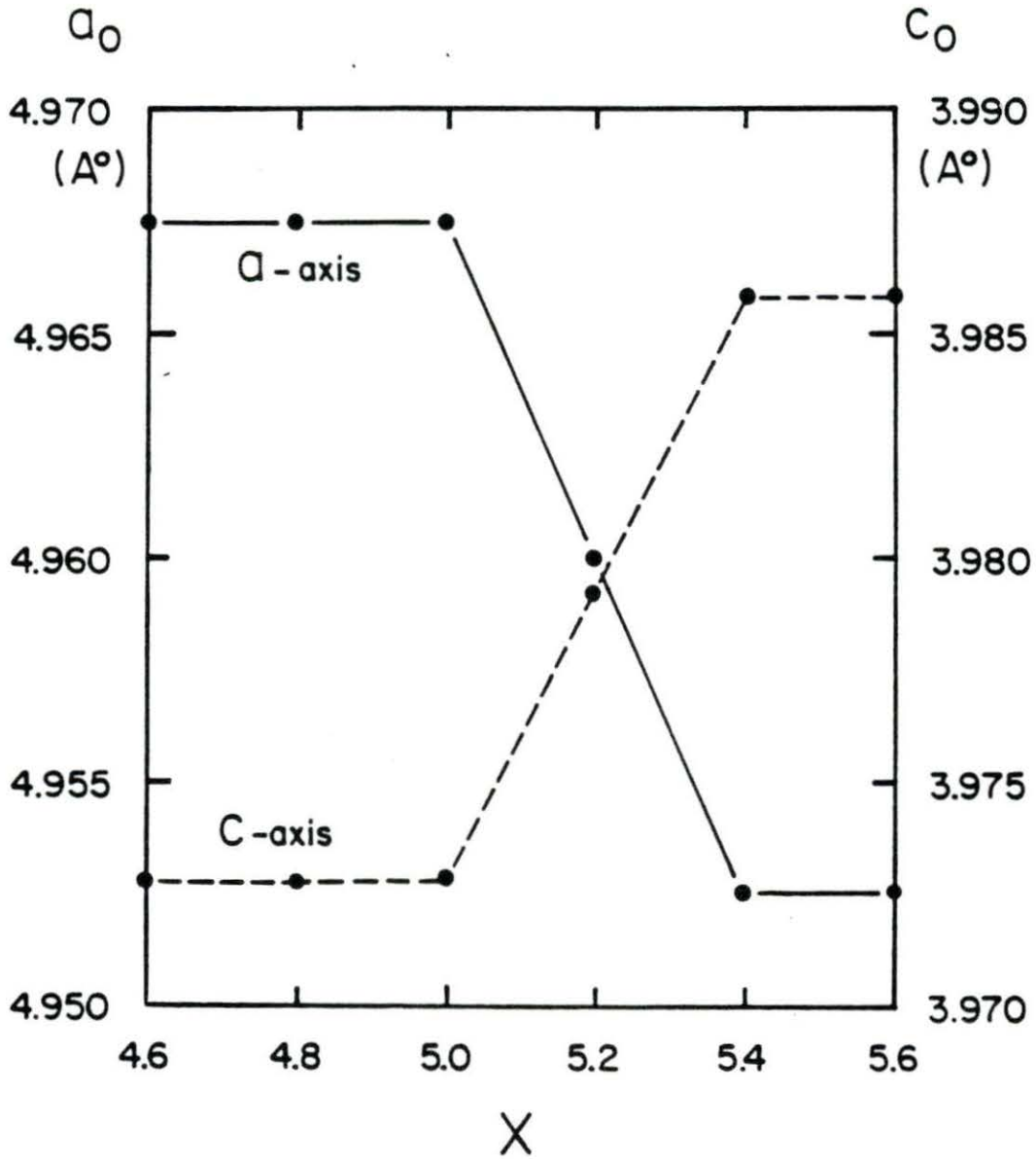Figure 13. Metallography of PrNi$_{5.2}$ quenched from 1100°C
(x250)

Figure 14. Composition dependence of a_o and c_o of $PrNi_x$ which were quenched from $1000°C$

tioned above, the $PrNi_{5.0}$ and $PrNi_{5.2}$ which were quenched from 1000°C are single phase alloys. Within the single phase region, the unit cell dimensions decrease in the $\underline{a}o$ direction but increase in the $\underline{c}o$ direction with increasing Ni concentration. The total unit cell volume, however, decreases with higher Ni concentration. These x-ray results are consistent with our observations. It is seen that within the homogeneous region an increase in Ni concentration results in increase in the room temperature resistivity.

V. DISCUSSION

As shown in Figure 14, the unit cell dimensions de-
crease in the $\underline{a}o$ direction but increase in the $\underline{c}o$ direction
when Ni concentration is increased. Such a peculiar varia-
tion of the lattice constants of a hexagonal $CaCu_5$ type com-
pounds was observed for $SmCo_5$ (21) and $LaNi_5$ (22). This
variation can be explained by a random substitution of a
pair of Ni atoms for some of the Pr atoms for x > 5.

The two substituted Ni atoms are arranged so that one
atom lies above and the other below the basal plane of the
$PrNi_5$ unit cell. This causes a contraction of the lattice
in the $\underline{a}o$ direction combined with an expansion in the $\underline{c}o$
direction.

Electrical resistivity depends primarily upon the
degree of freedom of motion of the conduction electrons
associated with a metallic crystal. A perfect periodic
metallic lattice should offer no resistance to the flow of
electricity at 0 K. Anything which perturbs the periodicity
of the lattice introduces a resistance to electron flow and
some of the energy of the moving electrons is converted in-
to increased atomic vibrations.

Atoms, in a pure crystal, which are not located pre-
cisely at lattice sites also constitute perturbations.
Therefore, lattice strains of any type such as those asso-

ciated with substitutional atoms or precipitate particles,
raise the electrical resistivity. As shown in Figure 12,
for $x \geq 5.2$ there are many precipitates at the grain boun-
daries and inside the grains. The increase in the resis-
tivity of the as-cast samples for $x \geq 5.2$ is partly due to
precipitates. Also, in the single phase region there is an
increase in electrical resistivity with the change of the
lattice dimensions with increasing Ni concentration. For
$x < 5$ and in the two phase region the residual resistivity
varies gradually with x, see Figure 6. Ott et al. (10)
have suggested that a slight excess of Pr is necessary to
completely fill the nickel d-band and suppress the s-d
scattering which is responsible for the large residual re-
sistivity for $x \geq 5.0$.

Generally, the resistivities of heat-treated samples
are slightly lower than those of as-cast samples, probably
because of the improved homogeneity in the heat-treated
samples.

PrNi$_x$ alloys are invariably brittle and sometimes
shattered when struck by the arc in the melting furnace.
These alloys are also hard to machine. Ott et al. (10)
found out that the thermal expansion of PrNi$_{5.0}$ is aniso-
tropic at low temperature. That is, with increasing tem-
perature the crystal expands perpendicular to the hexagonal

axis (in the basal plane) and a contraction is observed parallel to the six fold axis. Thus, c/a ratio decreases with increasing temperature. The magnitude of the expansion coefficient is extremely large as compared with normal metals. Therefore, to relieve the internal strains, cracks form on the initial cool down and this causes the resistivity to increase during first thermal cycling, and accounts for the different temperature dependence of the electrical resistivity for the cooling down.

There is probably a transition temperature from ductile to brittle behavior as the temperature decreases. Above the ductile-brittle transition thermal strains do not cause any microcracks to form because of the ductile nature of the materials, but below it cracks begin to develop. The ductile-brittle transition temperature is probably less than 300 K, because before the thermal cycling photomicrographs do not show any cracks. Cold stage microscopy should be able to pin-point this temperature.

VI. BIBLIOGRAPHY

1. Al'tshuler, S. A. JETP Letters 1966, 3, 112.

2. Andres, K.; Bucher, E. Phys. Rev. Letters 1968, 21, 1221.

3. Andres, K. Cryogenics 1978, 18, 473.

4. Nesbitt, E. A.; Williams, H. J.; Wernick, J. H.; Sherwood, R. C. J. Appl. Phys. 1962, 33, 1974.

5. Sugawara, T.; Terui, K.; Takayanagi, S. Japanese J. Appl. Phys. 1981, 20, 979.

6. Meijer, H. C.; Bots, G. J. C.; Postma, H. Physica 1981, 1·713, 607.

7. Andres, K.; Schmidt, P. H.; Darack, S. AIP Conf. Proc. 1974, 24, 238.

8. Andres, K.; Darack, S. Physica 1977, 86-88B, 1071.

9. Folle, H. R.; Kubota, M.; Buchal, C.; Mueller, R. M.; Pobell, F. Z. Phys. B - condensed matter 1981, 41, 223.

10. Ott, M. R.; Andres, K.; Bucher, E.; Maita, J. P. Solid State Comm. 1976, 18, 1303.

11. Wernick, J. H.; Geller, S. Acta Cryst. 1959, 12, 662.

12. Dwight, A. E. Trans. ASM 1961, 53, 477.

13. Mueller, R. M.; Buchal, C.; Folle, M. R.; Kubota, M.; Pobell, F. Cryogenics 1980, 395.

14. Reiffers, M.; Flachbart, K.; János, S.; Begnosov, A. B.; Eska, G. Phys. Stat. Sol. (b) 1982, 109, 369.

15. Craig, R. S.; Sankar, S. G.; Marzouk, V.; Rao, V. U. S.; Wallace, W. E.; Segal, E. J. Phys. Chem. Solids 1972, 33, 2267.

16. Meaden, G. T. "Electrical Resistance of Metals", Plenum: New York, 1965.

39

17. Lounasma, O. V. "Experimental Principles and Methods Below 1 K", Academic Press: New York, 1974.

18. Kittel, C. "Solid State Physics", John Wiley & Sons: New York, 1976.

19. Gschneidner, K. A., Jr. "Rare Earth Alloys", D. Van Nostrand: New York, 1961.

20. Gschneidner, K. A., Jr.; Eyring, L. "Handbook of the Physics and Chemistry of Rare Earths", North-Holland: Amsterdam, The Netherlands, 1978.

21. Buschow, K. H. J.; Van Der Goot, A. S. J. of Less-Common Metals 1968, 14, 323.

22. Buschow, K. H. J.; Van Mal, H. H. J. of Less-Common Metals 1972, 29, 203.

VII. ACKNOWLEDGMENTS